J Solid State Electrochem (2017) 21:1157–1164
DOI 10.1007/s10008-016-3458-2

ORIGINAL PAPER

The effect of ZnO addition on the electrochemical properties of the $LaNi_{3.55}Mn_{0.4}Al_{0.3}Co_{0.2}Fe_{0.55}$ electrode used in nickel–metal hydride batteries

Y. Dabaki[1] · S. Boussami[1] · C. Khaldi[1] · H. Takenouti[2,3] · O. ElKedim[4] · N. Fenineche[5] · J. Lamloumi[1]

Received: 16 June 2016 / Revised: 27 October 2016 / Accepted: 31 October 2016 / Published online: 17 November 2016

Abstract The studied electrochemical properties of the $LaNi_{3.55}Mn_{0.4}Al_{0.3}Co_{0.2}Fe_{0.55}$ alloy showed a rather poor performance. To improve them, ZnO, a doping agent at different small amounts (0, 1, or 2.5 wt%), was added to this base alloy. Then, the prepared electrodes were investigated by various electrochemical techniques. The maximum discharge capacity, obtained after the activation procedure, increased with the rise in ZnO content. The activation, as well as the reversibility of the hydrogen absorption/desorption process, were significantly improved with the addition of ZnO. It was observed that the latter did not affect considerably the stability and the cycling lifetime if added to the electrodes. After 30 charge/discharge cycles, the diffusion coefficients were estimated to be 1.55×10^{-11}, 1.30×10^{-11}, and 6.05×10^{-11} $cm^2\ s^{-1}$, respectively, for ZnO containing 0, 1, and 2.5 wt%. The ZnO catalyzed the kinetics of hydrogen absorption and desorption process thanks to capacity change before and after activation.

✉ C. Khaldi
chokri.khaldi@esstt.rnu.tn

[1] Equipe des Hydrures Métalliques, Laboratoire de Mécanique, Matériaux et Procédés, Ecole Nationale Supérieure d'Ingénieurs de Tunis (ENSIT (formerly ESSTT)), Université de Tunis, 5 Avenue Taha Hussein, 1008 Tunis, Tunisia

[2] Sorbonne Universités, UPMC Univ Paris 06, UMR 8235, Laboratoire Interfaces et Systèmes Electrochimique (LISE), Case 133, 4 place Jussieu, 75252 Paris CEDEX 05, France

[3] CNRS, UMR 8235, LISE, 4 place Jussieu, 75252 Paris CEDEX 05, France

[4] FEMTO-ST, MN2S, UTBM, Site de Sévenans, 90010 Belfort Cedex, France

[5] IRTES-LERMPS/FR FCLAB, UTBM, Site de Sévenans, 90010 Belfort Cedex, France

Keywords Ni–MH batteries · Catalyst · Electrochemical techniques · Redox kinetics · Intermetallic alloy

Introduction

The electrochemical discharge capacity of an intermetallic alloy, used as a negative electrode in Ni–MH batteries, depends mainly on its chemical composition and crystal structure. However, the grain fracturing as well as the alloy oxidation during cycling may change the kinetics of the hydrogen absorption and desorption processes [1–10]. Therefore, the alloy grain surface modification may also modify the electrode electrochemical properties often improved by mixing certain metal hydride powder with metal oxides [11, 12].

Iwakura et al. [13] reported that the addition of RuO_2, CoO, and Co_3O_4 to the $MmNi_{3.6}Mn_{0.4}Al_{0.3}Co_{0.7}$ alloy (where Mm stands for mischmetal) ameliorates significantly both the discharge capacity and the high-rate discharge ability.

Besides, Khrussanova et al. [14, 15] showed that the alloy mixture of Mg with some transition metal oxides (TiO_2, Fe_2O_3, MnO_2) catalyzes the hydrogen absorption and desorption kinetics. Oelerich et al. [16] also discussed the catalytic effects of different metal oxides on nanocrystalline Mg-based materials. They found that only the oxides of the transition metals, Ti, V, Cr, Mn, Fe, and Cu, having different valences, had a catalytic effect on the solid–gas reaction.

Actually, the electrochemical performances were improved significantly for the $Mg_{1.9}Y_{0.1}Ni_{0.9}Al_{0.12}$ electrode, after being mixed with 5 wt% of RuO_2 and V_2O_5 [17], and for nanocrystalline $LaMg_{12}Ni$ modified with a small amount of TiO_2 and Fe_3O_4 [18]. The AB_5-type alloys, modified with Bi_2O_3 [19] and CuO [20], also exhibited good electrochemical properties thanks to the reduction of these oxides to fine metal particles of Cu and Bi throughout cycling.

Zhang et al. [21] studied the influence of Fe_2O_3, TiO_2, Cr_2O_3, and ZnO addition at 5 wt% on the electrochemical properties of the $La_{1.3}CaMg_{0.7}Ni_9$ negative electrode. It improved significantly the maximum discharge capacity, high-rate discharge ability, and the exchange current density.

Li et al. [22] added the CuO oxide to the AB_3 metal hydride electrodes, in order to improve their electrochemical properties. The SEM observation and cyclic voltammogram show that the CuO can be reduced to fine Cu particles during charging, which will be deposited at the surface of the alloy particles. The as-deposited Cu particles form a protective layer to increase electronic and heat conductivity of the electrodes. Therefore, the improvement of the maximum discharge capacity, the high rate discharge-ability, the cycling stability and the high temperature discharge-ability of the electrodes is observed.

Su et al. [23] investigated the effect of Co_3O_4 addition on the electrochemical performance of metal hydride electrode. They showed that proper mass of Co_3O_4 can obviously improve the activation, the discharge capacity, the charge–discharge efficiency, high-rate discharge ability, cycle life, and high- and low-temperature capability. The performance measurement results proved that the high-rate discharge ability, inner pressure and overcharge endurance capability, temperature performance, and cycle lifetime of AA size cylindrical Ni–MH battery with Co_3O_4 as a negative additive were improved significantly. These results can be attributed to the high electrocatalytic activity and extended hydride storage capability of Co_3O_4, the improvement of gas consumption ability, and the restraining of oxidation of electrode alloys by adding Co_3O_4.

Li et al. [24] developed a simple method to fabricate the composite with nanosheet-shaped Co_3O_4 in situ growing on the surface of hydrogen storage alloys. Due to the enhanced catalytic activity of Co_3O_4 and the decreased internal resistance, the hydrogen absorption/desorption ability and electrochemical reaction kinetics are improved.

Since the electrochemical properties of the $LaNi_{3.55}Mn_{0.4}Al_{0.3}Co_{0.2}Fe_{0.55}$ alloy were deeply investigated [25, 26], we tried, in this work, to show if they can be improved by ZnO addition. In our study, the $LaNi_{3.55}Mn_{0.4}Al_{0.3}Co_{0.2}Fe_{0.55}$ alloy (hereby named the metal hydride electrode or anode during discharge) was mixed with different amounts of ZnO (0, 1, and 2.5 wt%). The catalytic effects of the different ZnO dopings on the electrochemical properties of the metal hydride electrode were also investigated.

Experimental procedures

The preparation and characterization of the metal hydride electrode under investigation were illustrated in our previous work [27, 28]. Then, the negative electrodes were prepared by a latex technology [29] after adding different amounts of ZnO (0, 1, and 2.5 wt%).

All the electrochemical measurements were performed at room temperature in a conventional three-electrode cell with a potentiostat–galvanostat EC-Lab® V10.12 system (BioLogic™). A nickel mesh and an Hg/HgO electrode were used as a counter electrode and a reference electrode, respectively. The electrolyte is a potassium hydroxide concentrated solution (1M KOH). It plays the role of an ionic conductor.

The activation procedure was realized through constant current charging and discharging at a C/10 rate. Indeed, the constant potential discharge (CPD) was applied after each cycle using a chronoamperometry method. The cyclic voltammetry (CV) tests were carried out at a scan rate of 1 mV s^{-1}, and the potential scan was performed from −1.3 to −0.60 V vs. Hg/HgO in order to estimate the exchange current density and the equilibrium potential (Nernst potential) in 1 M KOH solution.

Results and discussion

Activation and cycling of the metal hydride negative electrode prepared by adding ZnO

During the electrochemical cycling, a metal hydride electrode was activated when the next three conditions are fulfilled:

- The discharge capacity reaches its maximum value.
- The half-discharge potential becomes constant.
- The polarization, which is the difference between the potentials of half charge and half discharge of the alloy electrode, attains its minimum value and becomes constant independently of the cycling.

Figure 1 represents the discharge curves of the metal hydride anode during the first activation cycles prepared with the different added amounts of ZnO at C/10 rate: (a) 0, (b) 1, and (c) 2.5 wt%.

At the second cycle, the electrochemical discharge capacity are 92, 96, and 126 mAh g^{-1} and the potentials of half discharge are −770, −780, and −801 mV, respectively, for 0, 1, and 2.5 wt% ZnO added. At the fourth cycle, the capacity are 122, 138, and 178 mAh g^{-1} and the half-discharge potentials are −754, −785, and −800 mV, respectively, for 0, 1, and 2.5 wt% ZnO.

These discharge curves, relating to 0, 1, and 2.5 wt% ZnO, evolve, respectively, to achieve the maximum capacity values of 231 mAh g^{-1} at the 13th cycle, 223 mAh g^{-1} at the 8th cycle, and 247 mAh g^{-1} at the 7th cycle, and the potential of the corresponding half discharge becomes constant of −810, −785, and −782 mV with the appearance of an equilibrium plateau.

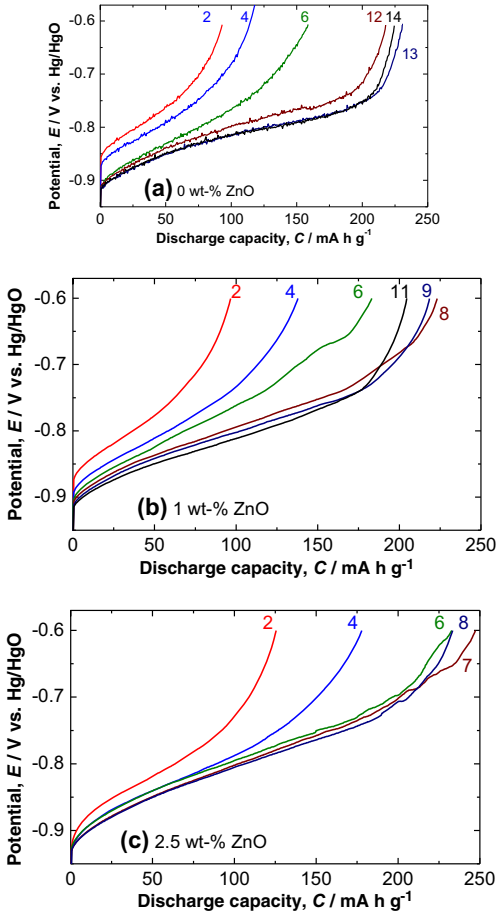

Fig. 1 Discharge curves of the metal hydride anode with different ZnO contents at C/10 rate during the first activation cycles: (**a**) 0 wt-%; (**b**) 1 wt-%; (**c**) 2.5 wt-% ZnO

The electrode, prepared without ZnO (0%), was activated after 13 cycles, while those prepared with 1 and 2.5 wt% ZnO were activated only after 8 and 7 cycles, respectively. Therefore, the activation process was significantly improved with the addition of ZnO.

Figure 2 depicts the evolution of the half-charge and discharge potentials of the metal hydride electrode prepared with different ZnO contents during the electrochemical cycling at C/10 rate.

To assess the reversibility of the charge and discharge reactions, we introduced the polarization parameter, expressed by the following equation:

$$\Delta E_{1/2} = E_{\frac{1}{2}\,\mathrm{charge}} - E_{\frac{1}{2}\,\mathrm{discharge}}$$

where $E_{\frac{1}{2}\,\mathrm{charge}}$ and $E_{\frac{1}{2}\,\mathrm{discharge}}$ are, respectively, the half-charge and half-discharge potentials.

The potential difference between the half-charge and discharge potentials, reflecting the reversibility of the charge and discharge reaction, is proportional to the ratio (expressed as a percentage) between the energy removed from a battery

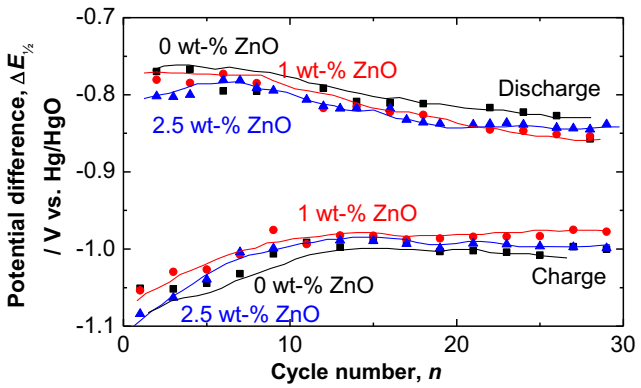

Fig. 2 Half-charge and discharge potentials of the metal hydride electrode, with different ZnO contents, during the electrochemical cycling at C/10 rate

during discharge compared with the energy used during charging to restore the original capacity, also called the coulombic efficiency or charge acceptance.

The polarization, defined as the difference between the half-charge and half-discharge potentials during the electrochemical cycling, decreased before stabilization regardless of the ZnO content. The polarization values after the stabilization are about 180, 126, and 150 mV for 0, 1, and 2.5 wt% ZnO, respectively. This result shows that the addition of ZnO improved the reversibility of the hydrogen absorption and the desorption reaction.

Figure 3 represents the maximum discharge capacity and polarization at C/10 rate according to the ZnO content of the metal hydride anode.

We find that the evolution of the maximum capacity with the content of ZnO is correlated with that of the polarization. The quantitative analysis of this evolution requires an examination by XRD of the different electrodes (0, 1, and 2.5 wt% ZnO), after the electrochemical measurements, to identify the amount of ZnO dissolved in the electrolyte and that undergoes a reduction in the form of Zn deposited on the electrodes.

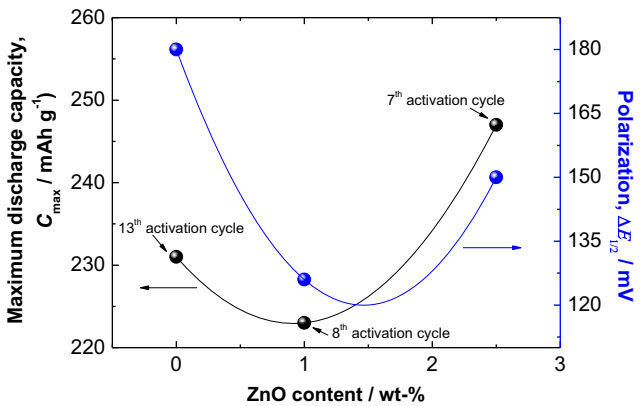

Fig. 3 Maximum discharge capacity at C/10 rate according to the ZnO content of the metal hydride anode

Figure 4 reveals the evolution of the electrochemical discharge capacity in function of the number of cycles for the metal hydride anode prepared with the different ZnO contents at C/10 rate.

The activation is defined by the maximum discharge capacity reached by cycling as shown in Table 1; it is obvious that the addition of ZnO is beneficial for the activation process. In fact, we notice that as the ZnO content increases, the decrease in the number of activation cycles is followed by a rise in the discharge capacity. In contrast, the latter, especially that containing higher ZnO content, is reduced at the 30th cycle to reach the maximum discharge capacity.

After activation, the electrochemical discharge capacity decreases in exponential-like law with respect to the cycle number. This decrease is more significant for the electrode containing high ZnO content. Indeed, the losses in discharge capacity after the 30th cycle are about 34, 40, and 49% for the 0, 1, and 2.5 wt% ZnO, respectively. Therefore, the increase in the ZnO amount added to the electrode does not improve its stability and cycling lifetime.

Zhang et al. [21] noticed that, according to an X-ray diffraction characterization of a ZnO-rich electrode, a progressive dissolution of ZnO into the KOH, explaining the catalytic effect of ZnO, can be maintained only during the first cycles.

The effect of ZnO addition on the kinetic properties of the metal hydride anode

First, the metal hydride electrodes, prepared with different ZnO contents, were fully charged under a constant current at C/10 rate. Then, it was discharged under a constant potential (−0.6 V vs. Hg/HgO).

Figure 5 shows the chronoamperograms of the metal hydride anode prepared with various ZnO amounts for different numbers of charge/discharge cycles.

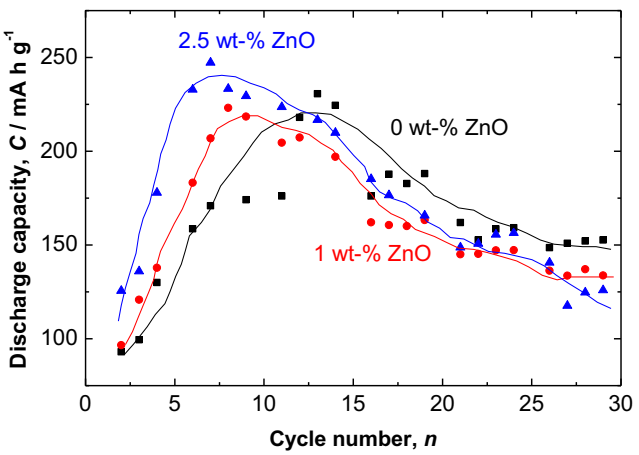

Fig. 4 Discharge capacity at C/10 rate according to the cycle number of the metal hydride anode prepared with different ZnO contents

Table 1 Activation cycle number, maximum discharge capacity, polarization, and the discharge capacity loss after 30 cycles of the metal hydride anode with different ZnO contents

ZnO content (wt%)	Activation cycle number	Q (mA h g^{-1})	$\Delta E_{1/2}$ (mV)	$100 \times \left(\frac{C_{max}-C_{30}}{C_{max}}\right)$ (%)
0	13	231	180	34
1	8	223	126	40
2.5	7	247	150	49

In this figure, we notice that the specific discharge current logarithm decreases linearly with time during a sufficiently large period [30]. This phenomenon resulted from the current density obtained from the diffusion process. It is expressed through the following equation:

$$\log(I) = \log\left[\pm\frac{6 \times F \times D_H}{d \times a^2}\left(C^0 - C_s\right)\right] - \frac{\pi^2 \times D_H}{\ln(10) \times a^2} \times t \quad (1)$$

where I stands for the specific discharge current density (A g^{-1}), a represents the average particle size of the alloy

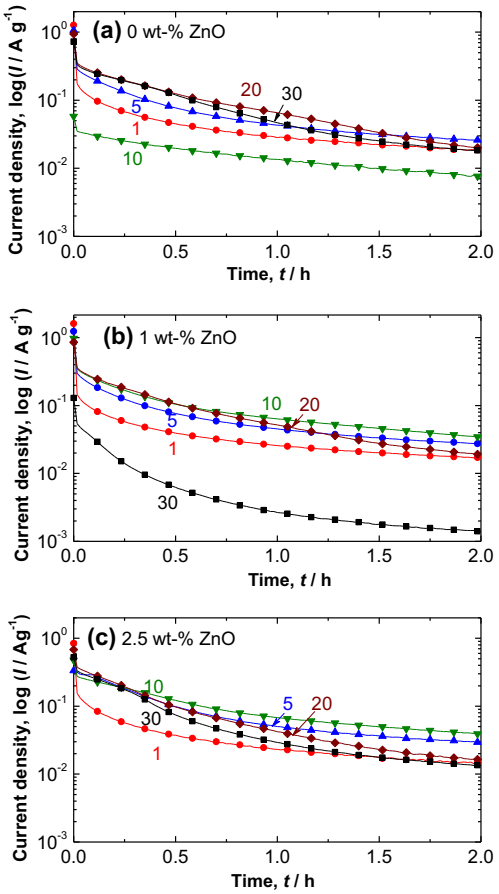

Fig. 5 Chronoamperograms of the metal hydride anode. **a** 0 wt%. **b** 1 wt%. **c** 2.5 wt% ZnO

considered as spherical (cm), D_H denotes the average value of the diffusion coefficient of the hydrogen in the electrode material (cm^2 s^{-1}), C^0 is the initial hydrogen concentration in the alloy bulk (mol cm^{-3}), C_s designates the hydrogen concentration on the vicinity of the alloy particle surface (mol cm^{-3}), F shows the Faraday (96,487 C mol^{-1}), d indicates the density of the hydrogen storage alloy (g cm^{-3}), and t represents the discharge time (s).

From the slope of the linear region of the corresponding plots, d(log(I))/d(t), the ratio of the metal hydride anode, D_H/a^2, prepared with different ZnO contents during the electrochemical cycling, was calculated as shown in Eq. (2):

$$\frac{D_H}{a^2} = -\frac{\ln(10)}{\pi^2}\frac{\mathrm{d}\log(I)}{\mathrm{d}\,t} \tag{2}$$

Figure 6 shows the D_H/a^2 ratio in function of the cycle number of the metal hydride anode with various ZnO contents.

All these curves have the same shape.

During the first activation cycles, the D_H/a^2 ratio undergoes a progressive increase before reaching its maximum value. The peaks of this ratio are 3.75 × 10^{-5}, 2.62 × 10^{-5}, and 2.28 × 10^{-5} s^{-1}, respectively, for 0, 1, and 2.5 wt% ZnO. The obtained result is in a good agreement with the increase of the discharge capacity during the first activation cycles. In a previous work [25], we showed that during the activation, the absorbed hydrogen by the alloy induced the electrode fracture and fissuring, leading to the consecutive increase of the active surface area.

After reaching its peak, the D_H/a^2 ratio gradually decreased due to the poor electrode cycling lifetime regardless of the ZnO content.

As shown in (Fig. 7), the average size of the intermetallic alloy particles was determined by scanning electron micrographs of the electrodes prepared with different ZnO contents after 30 cycles. In this figure, the average particle size, a, is estimated to be 9.2, 10.1, and 19.6 μm, respectively, for 0, 1, and 2.5 wt% ZnO. The diffusion coefficients of hydrogen will then be evaluated in Eq. (2) as 1.55 × 10^{-11}, 1.30 × 10^{-11}, and 6.05 × 10^{-11} cm^2 s^{-1}, respectively, for 0, 1, and 2.5 wt% ZnO.

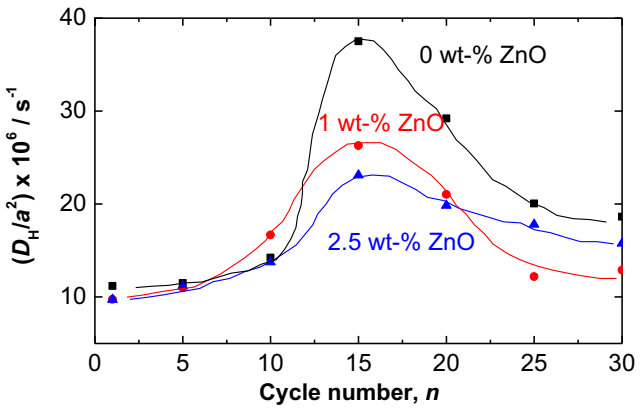

Fig. 6 The different D_H/a^2 ratios obtained according to the cycle number of the metal hydride anode prepared with various ZnO amounts

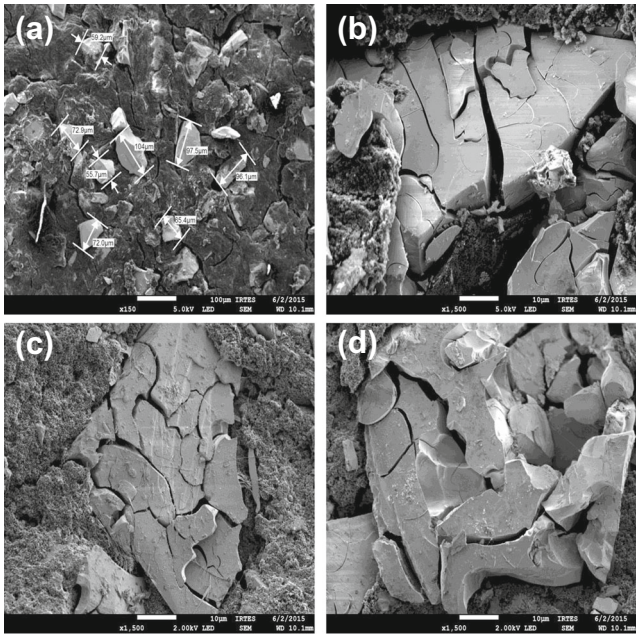

Fig. 7 SEM pictures of the intermetallic alloy prepared with different ZnO contents before cycling (**a**) and after 30 cycles at C/10 rates 0 (**b**), 1 (**c**), and 2.5% (**d**)

Redox properties of the metal hydride electrode with different ZnO contents

The redox behavior of the metal hydride electrode, prepared with different ZnO contents during 30 cycles and at room temperature, was studied using the linear voltammetry technique.

The voltammograms, obtained after each cycle, were treated and adjusted using origin software with the Butler–Volmer equation to determine the redox parameters. This method was depicted in our previous work [31, 32].

Figure 8 represents the evolution of the polarization curves during the cycling of the metal hydride electrodes prepared with different ZnO amounts. All the polarization curves, obtained during the first activation cycles, shift towards more positive potentials. This shift was faster for the ZnO-rich electrode, i.e., the insertion of hydrogen and the cathodic process, for the ZnO-rich electrode, became easier with the activation process as expected, leading to a more positive Nernst potential.

Figure 9 shows the evolution of the Nernst potential during the cycling of the metal hydride electrode with different ZnO contents.

During the activation, the Nernst potential of the ZnO-rich electrode move quickly towards the more positive

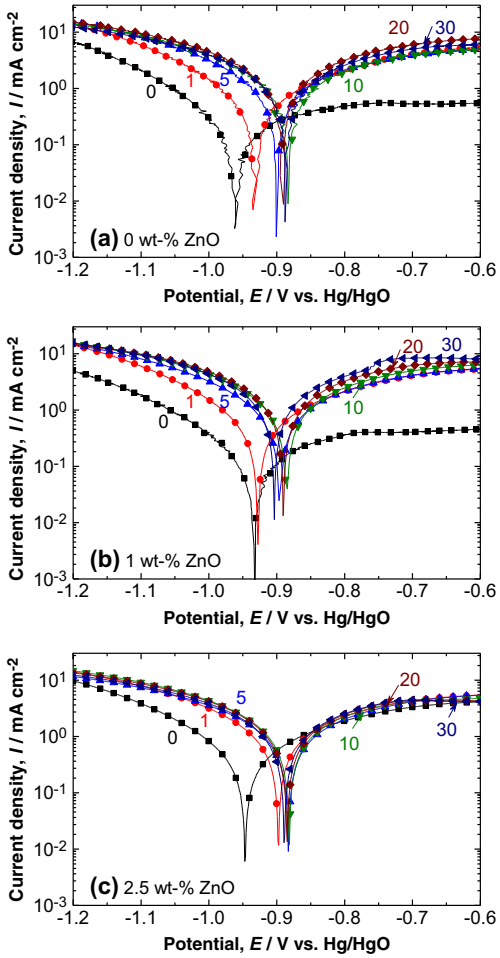

Fig. 8 Evolution of polarization curves during cycling of the metal hydride electrode with different ZnO contents. **a** 0 wt%. **b** 1 wt%. **c** 2.5 wt% ZnO

potential, i.e., the insertion of hydrogen becomes easier with activation process.

After activation, the Nernst potential of the ZnO-rich electrode move slowly towards the less positive potential

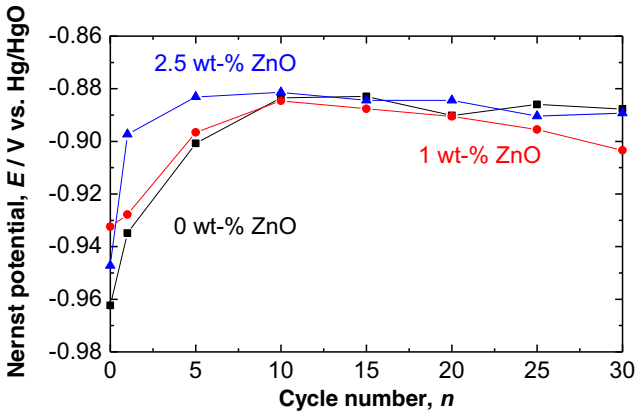

Fig. 9 Nernst potential change during cycling of the metal hydride anode, with different ZnO contents

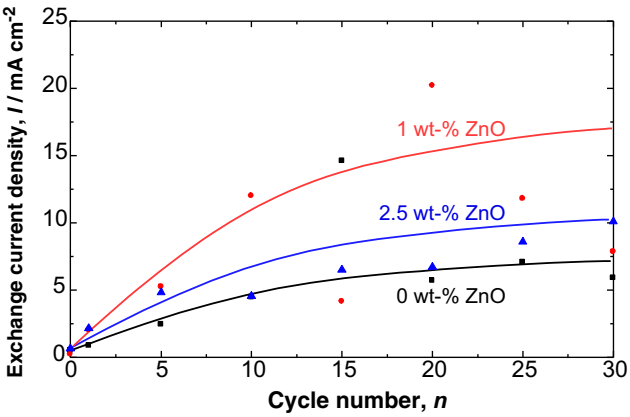

Fig. 10 Exchange current density I_0 during cycling of the metal hydride electrode with different ZnO contents

electrode, wherein the insertion of the hydrogen becomes more difficult.

Figure 10 reveals the exchange current density, I_0, during the cycling of the metal hydride electrode prepared with different ZnO contents.

Despite the few observed fluctuations, the exchange current density of the ZnO-containing electrode remained higher than that without ZnO. Therefore, the kinetics of hydrogen absorption and desorption was accelerated by adding ZnO as a catalyst.

This result was confirmed by magnetic measurements [33, 34] on an alloy of the same family, $LaNi_{3.55}Mn_{0.4}Al_{0.3}Fe_{0.75}$, rich in iron and without a catalytic substance.

Conclusion

The effect of the addition of metal oxide on the electrochemical hydrogen absorption and the desorption behavior of $LaNi_{3.55}Mn_{0.4}Al_{0.3}Co_{0.2}Fe_{0.55}$ alloy in 1 M KOH aqueous solution was investigated at room temperature through different electrochemical techniques. This intermetallic alloy was mixed with different amounts of ZnO up to 2.5 wt%.

The electrochemical characterization of the intermetallic alloys showed that:

- The electrode activation process was significantly improved with the addition of zinc oxide.
- The maximum discharge capacity, obtained after activation, increased as the ZnO content rises.
- The reversibility of the hydrogen absorption and desorption processes improved with the addition of ZnO.
- The increase of the D_H/a^2 ratio, during the first activation cycles, occurs along with the increase of the discharge capacity. After reaching its peak, the D_H/a^2 ratio gradually decreased due to the poor electrode cycling lifetime regardless of the ZnO content.

- The Nernst potential, provided during the first activation cycles, shifted towards a more positive direction. Indeed, with higher ZnO contents, the potential shift will be faster and the insertion of hydrogen of ZnO-rich electrode becomes easier. The increase of the cathodic and the hydrogen insertion processes made the Nernst potential more positive.
- The exchange current density corresponding to the electrodes containing ZnO remained greater than that without ZnO. Thus, the kinetics of hydrogen absorption and desorption were improved by ZnO addition as a catalyst.
- The redox process of hydrogen absorption and desorption can be enhanced by ZnO addition, along with the increase of discharge capacity before and after activation.

Acknowledgements The authors would like to express their gratefulness towards Mr. Latroche and Mrs. Percheron-Guégan (LCMTR, CNRS, France) for having offered to them the opportunity to prepare the alloys in their laboratory.

References

1. Hosni B, Li X, Khaldi C, Elkedim O, Lamloumi J (2014) Structure and electrochemical hydrogen storage properties of Ti_2Ni alloy synthesized by ball milling. J Alloys Compd 615:119–125
2. Boussami S, Khaldi C, Lamloumi J, Mathlouthi H, Takenouti H, Vivier V (2013) The impedance response of LaY_2Ni_9 negative electrode materials after activation. J Phys Chem Solids 74:1369–1374
3. Boussami S, Khaldi C, Lamloumi J, Mathlouthi H, Takenouti H (2012) Electrochemical study of $LaNi_{3.55}Mn_{0.4}Al_{0.3}Fe_{0.75}$ as negative electrode in alkaline secondary batteries. Electrochim Acta 69: 203–208
4. Khaldi C, Mathlouthi H, Lamloumi J (2009) A comparative study, of 1 M and 8 M KOH electrolyte concentrations, used in Ni–MH batteries. J Alloys Compd 469:464–474
5. Tliha M, Khaldi C, Mathlouthi H, Lamloumi J, Percheron-Guégan A (2007) Electrochemical investigation of the iron-containing and no iron-containing AB_5-type negative electrodes. J Alloys Compd 440:323–327
6. Tliha M, Mathlouthi H, Khaldi C, Lamloumi J Percheron-Guégan A (2006) Electrochemical properties of the $LaNi_{3.55}Mn_{0.4}Al_{0.3}Co_{0.4}Fe_{0.35}$ hydrogen storage alloy. J Power Sources 160: 1391–1394
7. Ben Moussa M, Abdellaoui M, Khaldi C, Mathlouthi H, Lamloumi J, Percheron-Guégan A (2005) Effect of substitution of Mm for La on the electrochemical properties of the $LaNi_{3.55}Mn_{0.4}Al_{0.3}Co_{0.75}$ compound. J Alloys Compd 399:264–269
8. Mathlouthi H, Khaldi C, Ben Moussa M, Lamloumi J, Percheron-Guégan A (2004) Electrochemical study of mono-substituted and poly-substituted intermetallic hydrides. J Alloys Compd 375:297–304
9. Khaldi C, Mathlouthi H, Lamloumi J, Percheron-Guégan A (2004) Electrochemical study of cobalt-free AB_5–type hydrogen storage alloys. Int J Hydrog Energy 29:307–311
10. Khaldi C, Boussami S, Ben Rejeb B, Mathlouthi H, Lamloumi J (2010) Corrosion effect on the electrochemical properties of $LaNi_{3.55}Mn_{0.4}Al_{0.3}Co_{0.75}$ and $LaNi_{3.55}Mn_{0.4}Al_{0.3}Fe_{0.75}$ negative electrodes used in Ni-MH batteries. Mater Sci Eng 175:22–28
11. Lee HJ, Yang DC, Park CJ, Park CN, Jang HJ (2009) Effects of surface modifications of the $LMNi_{3.9}Co_{0.6}Mn_{0.3}Al_{0.2}$ alloy in a $KOH/NaBH_4$ solution upon its electrode characteristics within a Ni–MH secondary battery. Int J Hydrog Energy 34:481–486
12. Angelo ACD (2006) Electrode surface modifications improve cathode hydrogen production and anode capacity in Ni–MH batteries. Int J Hydrog Energy 31:301–302
13. Iwakura C, Matsuoka M, Kohno T (1994) Mixing effect of metal oxides on negative electrode reactions in the nickel hydride battery. J Electrochem Soc 141:2306–2309
14. Khrussanova M, Terzieva M, Peshev P, Yu Ivanov E (1987) On the hydriding and dehydriding kinetics of magnesium with a titanium dioxide admixture. Mat Res Bull 22:405–412
15. Terzieva M, Khrussanova M, Peshev P (1991) Dehydriding kinetics of mechanically alloyed mixtures of magnesium with some 3d transition metal oxides. Int J Hydrog Energy 16:265–270
16. Oelerich W, Klassen T, Bormann R (2001) Metal oxides as catalysts for improved hydrogen sorption in nanocrystalline Mg-based materials. J Alloys Compd 315:237–242
17. Cui N, Luo JL (1998) Effects of oxide additions on electrochemical hydriding and dehydriding behavior of Mg_2Ni-type hydrogen storage alloy electrode in 6 M KOH solution. Electrochim Acta 44: 711–720
18. Wang Y, Gao XP, Lu ZW, Hu WK, Zhou Z, Qu JQ, Shen PW (2005) Effects of metal oxides on electrochemical hydrogen storage of nanocrystalline $LaMg_{12}$–Ni composites. Electrochim Acta 50: 2187–2191
19. Cheng SA, Lei YQ, Leng YJ, Wang QD (1998) Electrochemical performance of metal hydride negative electrode modified with bismuth oxide. J Alloys Compd 264:104–106
20. Zhang S, Shi P, Deng C (2006) Characteristics of hydrogen storage alloy electrode with cupric oxide additive. Solid State Ionics 177: 1193–1197
21. Zhang P, Wei X, Liu Y, Zhu J, Yu G (2008) Effects of metal oxides addition on the performance of $La_{1.3}CaMg_{0.7}Ni_9$ hydrogen storage alloy. Int J Hydrog Energy 33:1304–1309
22. Li Y, Han S, Zhu X, Ding H (2010) Effect of CuO addition on electrochemical properties of AB_3-type alloy electrodes for nickel/metal hydride batteries. J Power Sources 195:380–383
23. Su G, He YH, Liu KY (2012) Effects of Co_3O_4 as additive on the performance of metal hydride electrode and Ni–MH battery. Int J Hydrogen Energy 37:11994–12002
24. Li MM, Yang CC, Jing WT, Jin B, Lang XY, Jiang Q (2016) In situ grown Co_3O_4 on hydrogen storage alloys for enhanced electrochemical performance. Int J Hydrog Energy 41:8946–8953
25. Khaldi C, Mathlouthi H, Lamloumi J, Percheron-Guégan A (2004) Electrochemical impedance spectroscopy and constant potential discharge studies of $LaNi_{3.55}Mn_{0.4}Al_{0.3}Co_{0.75-x}Fe_x$ hydrides alloy electrodes. J Alloys Compd 384:249–253
26. Khaldi C, Mathlouthi H, Lamloumi J, Percheron-Guégan A (2003) Effect of partial substitution of Co with Fe on the properties of $LaNi_{3.55}Mn_{0.4}Al_{0.3}Co_{0.75-x}Fe_x$ (x = 0, 0.15, 0.55) alloys electrodes. J Alloys Compd 360:266–271
27. Ayari M (2003) Etude des propriétés des composes $LaNi_{3.55}Mn_{0.4}Al_{0.3}Co_{0.75-x}Fe_x$–Application aux accumulateurs Ni-MH. Thèse d'Université, Faculté des Sciences de Tunis
28. Mathlouthi H, Lamloumi J, Latroche M, Percheron-Guégan A (1997) Study of poly-substituted intermetallic hydrides: electrochemical applications. Ann Chim Sci Mater 22:241–244
29. Li CJ, Wang FR, Cheng WH, Li W, Zhao WT (2001) The influence of high-rate quenching on the cycle stability and the structure of the AB_5-type hydrogen storage alloys with different Co content. J Alloys Compd 315:218–223
30. Khaldi C (2004) Contribution à l'étude des propriétés physico-chimiques des alliages $LaNi_{3.55}Mn_{0.4}Al_{0.3}Co_{0.75-x}Fe_x$ (x =0, 0.15,

0.55, 0.75)-application aux accumulateurs nickel–metal-hydrure. Thèse d'Université, Faculté des Sciences de Tunis
31. Khaldi C, Boussami S, Tliha M, Azizi S, Fenineche N, El-Kedim O, Mathlouthi H, Lamloumi J (2013) The effect of the temperature on the electrochemical properties of the hydrogen storage alloy for nickel–metal hydride accumulators. J Alloys Compd 574:59–66
32. Bard AJ, Faulkner LR (2001) Electrochemical methods: fundamentals and applications, 2nd edn. John Wiley & Sons
33. Ayari M, Paul-Boncour V, Lamloumi J, Percheron-Guégan A (2003) Decomposition of the $La_{3.55}Ni_{0.4}Al_{0.3}Fe_{0.75}$ compound upon electrochemical cycling studied by magnetic properties. J Alloys Compd 356–357:133–136
34. Ayari M, Paul-Boncour V, Lamloumi J, Percheron-Guégan A, Guillot M (2005) Study of the aging of $LaNi_{3.55}Mn_{0.4}Al_{0.3}(Co_{1-x}Fe_x)_{0.75}$ ($0 \leq x \leq 1$) compounds in Ni–MH batteries by SEM and magnetic measurements. J Magn Magn Mater 288:374–383